

# Chiral topological spin liquids with projected entangled pair states

Didier Poilblanc,<sup>1</sup> J. Ignacio Cirac,<sup>2</sup> and Norbert Schuch<sup>3</sup>

<sup>1</sup>*Laboratoire de Physique Théorique, C.N.R.S. and Université de Toulouse, 31062 Toulouse, France*

<sup>2</sup>*Max-Planck-Institut für Quantenoptik, Hans-Kopfermann-Str. 1, D-85748 Garching, Germany*

<sup>3</sup>*Institut für Quanteninformatik, RWTH Aachen, D-52056 Aachen, Germany*

(Dated: July 10, 2015)

Topological chiral phases are ubiquitous in the physics of the Fractional Quantum Hall Effect. Non-chiral topological spin liquids are also well known. Here, using the framework of projected entangled pair states (PEPS), we construct a family of chiral spin liquids on the square lattice which are generalized spin-1/2 Resonating Valence Bond (RVB) states obtained from deformed local tensors with  $d + id$  symmetry. On a cylinder, we construct four topological sectors with even or odd number of spinons on the boundary and even or odd number of ( $\mathbb{Z}_2$ ) fluxes penetrating the cylinder which, we argue, remain orthogonal in the limit of infinite perimeter. The analysis of the transfer matrix provides evidence of short-range (long-range) triplet (singlet) correlations as for the critical (non-chiral) RVB state. The Entanglement Spectrum exhibits chiral edge modes, which we confront to predictions of Conformal Field Theory, and the corresponding Entanglement Hamiltonian is shown to be long ranged.

PACS numbers: 75.10.Kt, 75.10.Jm

*Introduction* – The study of topological states of matter is the focus of research of a multidisciplinary scientific community. On the one hand, they give rise to very exotic behavior associated to the topological order [1], something which has no analog in standard Condensed Matter Physics. On the other, it provides an alternative and promising approach to fault tolerant quantum computing [2]. Furthermore, experiments both with new materials [3] and cold atoms [4] are now at the position of engineering some of those states, and thus provide a laboratory to verify the theoretical findings.

Two of the main theoretical challenges in the study of topological matter are the identification of simple models and descriptions which can lend us a complete understanding of their exotic properties, as well as the derivation of parent Hamiltonians, so that we get a hint of how to create the states, or under which conditions we can find them at low temperature. A possible approach to attack both challenges is through the use of tensor networks, and in particular of Projected Entangled Pair States (PEPS) [5, 6]. They provide a simple local description of many body states from which their physical properties can be determined, and they imply the existence of a parent local Hamiltonian.

So far, most of the PEPS studies have concentrated on non-chiral topologically ordered states, like the toric code [2, 6], double and Levin-Wen models [7], or the short-range spin-1/2 RVB states [8–11]. The latter is specially appealing as it respects  $su(2)$  symmetry and is translationally invariant, something which naturally appears in many materials [12]. Furthermore, in the Kagome lattice it corresponds to a  $\mathbb{Z}_2$  spin liquid [9, 10], with very well known anyonic excitations.

Another class of topological ordered matter corresponds to the Fractional Quantum Hall State (FQHS)

exhibiting protected chiral edge modes [13] that are fully characterized by a chiral CFT [14]. For example, the edge states of the bosonic Laughlin [15], Moore-Read [16] and Read-Rezayi [17] states can be described by a chiral  $SU(2)_k$  CFT of the Wess-Zumino-Witten (WZW) model [14], where  $k = 1; 2$  and  $3$  respectively. The edge modes are protected by the long-range topological order of the bulk which hosts quasiparticles (or anyons) with Abelian ( $k = 1$ ) and non-Abelian ( $k > 1$ ) fractional statistics. Recently, an emergent topological chiral spin liquid (CSL), similar to the one proposed by Kalmeyer and Laughlin (KL) [18, 19], has been discovered in the Kagome quantum antiferromagnet with broken time-reversal (TR) symmetry [20] as well as in the square lattice [21], realizing the spin analogue of the bosonic Laughlin state. A FQHS was also found in a TR invariant Kagome Heisenberg model [22]. Whether PEPS can be derived for gapped chiral phases of interacting systems remains a major and subtle issue debated in recent papers [23, 24]. Nevertheless, a critical chiral PEPS with topological order has been constructed by Gutzwiller projecting two copies of chiral states of free fermions [25]. Using the PEPS bulk-edge correspondence, the edge CFT could be identified as  $SO(2)_1$  but with an infinite correlation length.

In this paper we show that by deforming the tensors corresponding to the RVB spin-1/2 state, implementing  $d + id$  symmetry, one can break the TR symmetry but keeping the  $su(2)$  and other symmetries of the state, and obtain a chiral topological state. We analyze the topological degeneracies, the entanglement spectrum and the entropy via the bulk-boundary correspondence. The chiral edge modes bear some features of CFT although a precise identification to simple known CFT was not possible. We work on a square lattice, and find that, as

the RVB state [26, 27], the family we construct has infinite correlation length and, hence, moves along a critical phase of a local Hamiltonian.

*PEPS framework* – We consider a two-dimensional (2d) bipartite square lattice where a rank-5 tensor  $A_{lurd}^s$  of dimension  $dD^4$  is assigned to each site. Here, the index  $s = 0, 1$  stands for the local physical spin-1/2 degrees of freedom (of dimension  $d = 2$ ) and the subscript indices  $l, u, r, d$  label the virtual states on the four bonds as shown in Fig. 1(a). Basically, we can write a general spin-1/2 ansatz wave function on a periodic manifold of  $M$  sites as  $|\Psi\rangle = \sum_{s_1, s_2, \dots, s_M} c_{s_1, s_2, \dots, s_M} |s_1, s_2, \dots, s_M\rangle$ , and  $c_{s_1, s_2, \dots, s_M} = \text{Contract}[A^{s_1} A^{s_2} \dots A^{s_M}]$  where all tensors share the same bond variables with their 4 neighbors and “Contract” means that one sums up over all bond variables of the 2d tensor network. In order to construct a generalized spin-singlet RVB wavefunction, we assume that the virtual states belong to the  $1/2 \oplus 0$  spin representation of dimension  $D = 3$  (the virtual states  $|\uparrow\rangle, |\downarrow\rangle$  and  $|0\rangle$  carry  $S_z = 1/2, -1/2$  and  $0$ , respectively) [9, 10]. Since in each configuration of the RVB state, exactly one bond singlet  $|\uparrow\downarrow\rangle - |\downarrow\uparrow\rangle$  is connected to each lattice site, the precise sign structure of the RVB state depends on the orientations of the latter: hereafter singlets are oriented from one sublattice (A) to the other sublattice (B) as shown in Fig. 1(b). After a 180-degree spin-rotation on the B sites (see Fig. 1(c)) the RVB state takes the form of a translationally invariant PEPS with *the same* tensor on both sublattices. Whenever open boundaries are present, one needs to assign the values of the non-contracted virtual indices at the boundaries to fully characterize the PEPS wave function.

*Chiral RVB* – Our goal is to find a PEPS representation of a family of states  $\Psi$  with  $\text{su}(2)$ , 90 degree rotation and translational symmetry, and that contains the RVB state on a square lattice. More precisely, let us define by  $G_i$  the group transformations of  $C_{4v}$  corresponding to reflection along the vertical, horizontal, and 45 degrees axis. We want to impose that  $G_i|\Psi\rangle$  coincides with  $|\Psi^*\rangle$ . For PEPS, one can enforce this symmetry at the level of the tensor  $A$  itself. This constraint, together with the additional ones imposed by the singlet character of the PEPS fully determine the tensor  $A$  in terms of three real parameters (see Appendix):

$$A = \lambda_1 R_1 + \lambda_2 R_2 + i\lambda_{\text{chiral}} I, \quad (1)$$

where the (real)  $R_a$  and  $I$  tensors transform according to the  $B_1$  and  $B_2$  irreducible representations (IRREP) of  $C_{4v}$  [28, 29], respectively. In other words, the  $A$  tensor has  $d + id$  (meaning  $d_{x^2-y^2} + id_{xy}$ ) symmetry. On a finite  $L \times L$  torus with an even number of sites, the real (imaginary) parts of the PEPS are sums of products of even (odd) numbers of  $R$  by even (odd) numbers of  $I$  tensors. Therefore, the PEPS takes the form,  $\Psi = \Psi_s + i\Psi_g$ , where the real components  $\Psi_s$  and  $\Psi_g$  transform according to the  $A_1$  ( $s$ -wave) and  $A_2$  ( $g$ -wave) IRREP, respec-

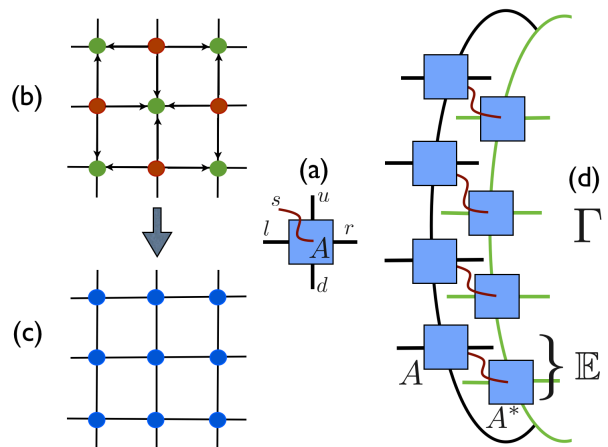


FIG. 1: (a) Local tensor  $A$ . (b) Square lattice with (nearest-neighbor) singlet bonds oriented from sublattice A to sublattice B. (c) Under a 180-degree spin rotation on e.g. the B sublattice, oriented singlets are transformed into symmetric  $|\uparrow\uparrow\rangle + |\downarrow\downarrow\rangle$  maximally entangled pair states. (d) Transfer matrix on a periodic ring connecting the (non-contracted) BK virtual indices on the left of the ring to the ones on its right.

tively, so that  $G_i|\Psi_s\rangle = |\Psi_s\rangle$  and  $G_i|\Psi_g\rangle = -|\Psi_g\rangle$ . For  $\lambda_2 = \lambda_{\text{chiral}} = 0$ , one recovers the simple nearest-neighbor RVB state [9, 10].  $\lambda_2$  and  $\lambda_{\text{chiral}}$  introduce longer range (AB) singlet bonds via “teleportation” as in the non-chiral spin liquid of Ref. 11. Note that we found that  $|\Psi_g\rangle \neq 0$  only if  $\lambda_2 \neq 0$  and  $\lambda_{\text{chiral}} \neq 0$  simultaneously. Hereafter we fix  $\lambda_1 = \lambda_2 = 1$ .

In order to identify the above PEPS as a chiral spin liquid with topological order we have to prove that (i)  $\Psi$  and  $\Psi^*$  are different in the thermodynamic limit and (ii) there are different topological sectors on a cylinder e.g. with even or odd number of spinons on the boundaries or with even or odd number of ( $\mathbb{Z}_2$ ) fluxes penetrating the cylinder. (iii) In addition, we have to fully characterize the edge physics using the PEPS bulk-boundary correspondence, so that we can determine the Entanglement Spectrum (ES) and the Entanglement Entropy (EE).

*Transfer matrix and topological sectors* – To do so we place the PEPS wavefunctions  $\Psi$  and  $\Psi^*$  on a (horizontal) cylinder of circumference  $N_v$  ( $= 4, 6, 8$ ) and length  $N_h \rightarrow \infty$ . Their overlap can be written as a bracket (BK) product  $\langle \Psi | \Psi^* \rangle = V_{\text{left}} \tilde{\Gamma}^{N_h} V_{\text{right}}$  where  $\tilde{\Gamma}$  is a  $D^{2N_v} \times D^{2N_v}$  transfer matrix (TM) and  $V_{\text{left}}$  and  $V_{\text{right}}$  stand for left and right vectors (of dimension  $D^{2N_v}$ ) defining the boundary conditions. To construct  $\tilde{\Gamma}$  one first defines a local rank-4  $\mathbb{E}$  tensor by contracting the physical index of two superposed bra and ket  $A$  tensors, namely  $\tilde{\mathbb{E}}_{LURD} = \sum_s A_{lurd}^s A_{l'u'r'd'}^s$  where the indices of  $\mathbb{E}$  combine the indices of the superposed bonds of the top (bra) and bottom (ket)  $A$  tensors. Then, one builds a (vertical) periodic array of  $N_v$  such  $\mathbb{E}$  tensors, contracting over the (vertical) bond indices as shown in Fig. 1(d). Similarly, one can also construct the “regular” transfer

matrix  $\Gamma$  as  $\mathbb{E}_{LURD} = \sum_s A_{lurd}^s (A_{l'u'r'd'}^s)^*$  from which the normalization  $\langle \Psi | \Psi \rangle$  can be obtained. If the leading eigenvalue (LE)  $\tilde{\gamma}_{ee}$  of  $\tilde{\Gamma}$  (normalized by the LE of  $\Gamma$ ) is strictly smaller than 1, then  $\Psi$  and  $\Psi^*$  are orthogonal in the  $N_h \rightarrow \infty$  limit. This is what is observed in Figs. 2(a) as soon as  $\Psi$  acquires an imaginary component. Also, for increasing circumference,  $\tilde{\gamma}_{ee} \rightarrow 0$  as seen in Fig. 2(b), implying that  $\Psi$  and  $\Psi^*$  are indeed two independent states.

Topological properties of  $\Psi$  (topological sectors, etc...) can be obtained from the “regular” TM [30]. It is easy to check that  $\Gamma$  (like  $\tilde{\Gamma}$ ) has a simple block-diagonal structure associated to a number of conserved quantities like the difference  $S_z^{BK} = S_z^{\text{bra}} - S_z^{\text{ket}}$  between the  $z$ -components of the total virtual spin [31] on the bra and the ket, namely  $\Gamma = \bigoplus \Gamma[S_z^{BK}]$ . We found that the leading eigenvalues of the TM’s appear in the lowest  $S_z^{BK}$  sectors, namely  $S_z^{BK} = 0$  and  $S_z^{BK} = \pm 1/2$ . Secondly, one finds that the parity of the number of virtual  $|0\rangle$  states (or spinons at the boundaries) is conserved *independently* in the bra (top) and ket (bottom) layers, as for the Kagome RVB  $\mathbb{Z}_2$  liquid [9, 10, 32], suggesting topological order. The  $S_z^{BK} = 0$  sector of  $\Gamma$  is therefore split into even-even (ee) and odd-odd (oo) sub-sectors, namely  $\Gamma[0] = \Gamma_{ee} \oplus \Gamma_{oo}$ , while the  $S_z^{BK} = 1/2$  sector is split into two degenerate even-odd (eo) and odd-even (oe) sub-sectors, namely  $\Gamma[1/2] = \Gamma_{eo} \oplus \Gamma_{oe}$ . In addition, one can insert (horizontal) strings of  $\mathbb{Z}_2$  vison operators [9, 10] in the bra and/or ket layers of  $\Gamma$  (restricting here to  $\Gamma_{ee}$ ). We found that the resulting TM depend only on the *parities* of the number of  $\pi$ -fluxes in each layer. We denote by  $\Gamma_{\pi_0}$  ( $\Gamma_{\pi\pi}$ ) the TM with a vison flux in a single (both) layer(s).

From the above analysis we see that, a priori, one can construct four wave functions  $\Psi_e^0$ ,  $\Psi_o^0$ ,  $\Psi_e^\pi$  and  $\Psi_o^\pi$  characterized by the parities of the numbers of spinons at the boundary (as specified by the subscript) and fluxes penetrating the cylinder (as specified by the superscript). However, we still have to check that these wave functions, locally indistinguishable, remain truly distinct (and hence orthogonal) in the thermodynamic limit. For  $N_h \gg N_v$ , the overlaps behave as  $\langle \Psi_o^0 | \Psi_e^0 \rangle = (f_{eo})^{N_h}$  and  $\langle \Psi_e^\pi | \Psi_o^\pi \rangle = (f_{\pi o})^{N_h}$  with  $f_{eo} = \gamma_{eo} / (\gamma_{ee} \gamma_{oo})^{1/2}$  and  $f_{\pi o} = \gamma_{\pi o} / (\gamma_{ee} \gamma_{\pi\pi})^{1/2}$ , where  $\gamma_{ee}$ ,  $\gamma_{oo}$ ,  $\gamma_{\pi\pi}$ ,  $\gamma_{eo}$ , and  $\gamma_{\pi o}$  are the LE of  $\Gamma_{ee}$ ,  $\Gamma_{oo}$ ,  $\Gamma_{\pi\pi}$ ,  $\Gamma_{eo}$ , and  $\Gamma_{\pi o}$ , respectively. If the wave function subspace remains degenerate in the  $N_v \rightarrow \infty$  limit, we expect that (i)  $\gamma_{oo}$  and  $\gamma_{\pi\pi}$  converge exactly to  $\gamma_{ee}$  (the largest LE set to 1) while (ii)  $f_{eo}$  and  $f_{\pi o}$  converge to values *strictly smaller than 1*. In contrast, if  $f_{\pi o} \rightarrow 1$  (or  $f_{eo} \rightarrow 1$ ), the insertion of a flux in the cylinder (or a spinon at the boundaries) does not generate a new topological sector. The finite size scalings shown in Fig. 2(b) – or in the Appendix for other parameters – are all compatible with (i). However, extrapolations of either  $f_{\pi o}$  or  $f_{eo}$  might be inaccurate in some cases – see Fig. 2(b) and Appendix for other pa-

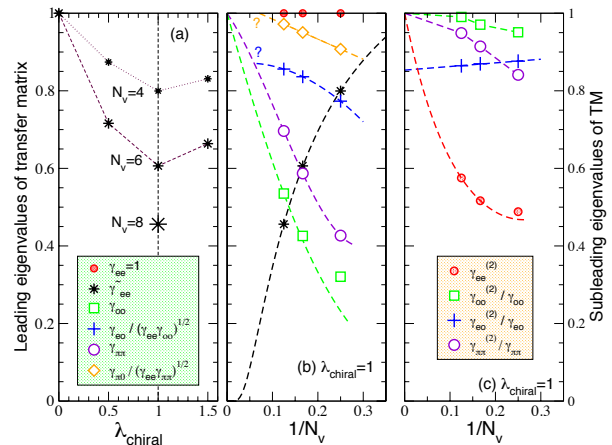


FIG. 2: (a) Leading eigenvalue  $\tilde{\gamma}_{ee}$  (normalized by  $\gamma_{ee}$ ) of the  $\tilde{\Gamma}_{ee}$  block of the transfer matrix as a function of  $\lambda_{\text{chiral}}$  (for  $\lambda_1 = \lambda_2 = 1$ ) and for  $N_v = 4, 6$  and  $8$  (as shown on plot). (b) Finite size scaling of the leading eigenvalues of the diagonal blocks ( $\Gamma_{ee}$  and  $\Gamma_{oo}$ ) and of the off-diagonal blocks ( $\tilde{\Gamma}_{ee}$  and  $\Gamma_{eo}$ ) of the transfer matrix (after proper normalization). The diagonal (off-diagonal) blocks have  $S_z^{BK} = 0$  ( $S_z^{BK} = 1/2$ ) quantum numbers. (c) Finite size scaling of the second leading eigenvalues  $\gamma_{\mu\nu}^{(2)}$  of the  $\Gamma_{ee}$ ,  $\Gamma_{oo}$  and  $\Gamma_{eo}$  blocks (after proper normalization).

rameters – due to slow convergence and the limitation to small perimeters. It is however plausible that  $f_{eo} < 1$  and  $f_{\pi o} < 1$  in the thermodynamic limit (at least for some parameters) ensuring the existence of four Indentity ( $\Psi_e^0$ ), Spinon ( $\Psi_o^0$ ), Vison ( $\Psi_e^\pi$ ) and Vison/Spinon ( $\Psi_o^\pi$ ) topological sectors (wave functions).

*Asymptotic correlations* – The behavior of the second LE  $\gamma_{\mu\nu}^{(2)}$  (to be normalized by the leading one) of each block  $\Gamma_{\mu\nu}$  of  $\Gamma$ , provides key informations on the long-distance correlations associated to the quantum number of the block – typically one expects  $\gamma_{\mu\nu}^{(2)} / \gamma_{\mu\nu} \sim \exp(-1/\xi_{\mu\nu})$ . The finite size scalings shown in Fig. 2(c) suggest that both  $\gamma_{ee}^{(2)} \rightarrow 1$  and  $\gamma_{oo}^{(2)} / \gamma_{oo} \rightarrow 1$ . We also find that the next LE are also going to 1, an evidence of gapless even-even and odd-odd sectors of the TM i.e.  $\xi_{ee} = \xi_{oo} = \infty$ . Correlations of spin-singlet operators are therefore expected to be algebraic (infinite correlation length). In contrast, we find a gapped even-odd sector with an extrapolated value  $\gamma_{oe}^{(2)} / \gamma_{oe} |_{\infty} \simeq 0.85$  corresponding to a magnetic correlation length  $\xi_{eo} \sim 6$  (in units of the lattice spacing) for  $\lambda_{\text{chiral}} = 1$ .

*Entanglement Spectrum and chiral edge modes* – Using the standard procedure [6], we have computed the ES, EE and Entanglement Hamiltonian (EH) for infinite cylinders (of circumference  $N_v = 4, 6$  and  $8$ ) cut into two (semi-infinite) halves. The fixed-point right and left vectors,  $V_R^{\mu\mu}$  and  $V_L^{\mu\mu}$  obtained by applying the TM iteratively on (random) boundary vectors belonging to the  $S_z^{BK} = 0$  even ( $\mu \equiv e$ ) and odd ( $\mu \equiv o$ ) sectors are

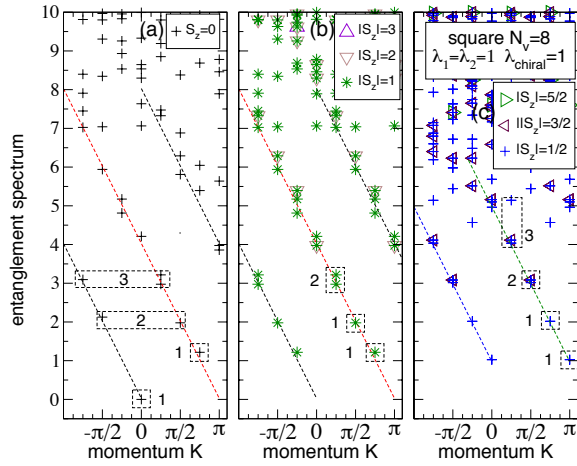


FIG. 3: Re-scaled Entanglement Spectrum vs momentum along the edge (for  $\lambda_1 = \lambda_2 = \lambda_{\text{chiral}} = 1$ ). (a), (b) and (c) show different sectors of the Z-component of the virtual spin on the edge. The dashed lines show the chiral edge modes. In (a), the momentum of the states of the chiral mode is defined mod  $\pi$ . The multiplicities 1, 1, 2, and 3 of the quasi-degenerate states in the boxes – expected for a CFT – are shown on the plot.

viewed as operators (of trace 1) acting on the virtual indices at the edge. From the right and left operators  $\sigma_L = \frac{1}{2}(V_L^{ee} + V_L^{oo})$  and  $\sigma_R = \frac{1}{2}(V_R^{ee} + V_R^{oo})$ , one obtains the EH  $H_E = -\ln(\sqrt{(\sigma_R)^T} \sigma_L \sqrt{(\sigma_R)^T})$ .  $H_E$  is block-diagonal and the blocks are labelled by the momentum  $K$  along the edge and by the modulus of the z-component of the virtual (edge) spin  $|S_z| = |S_z^{\text{bra}}| = |S_z^{\text{ket}}|$  [31]. We have computed the ES on infinite cylinders as a function of  $K$ . At low (quasi)energy, linearly dispersing chiral (i.e. with a definite sign of their velocity) modes with almost equally spaced levels are seen for all values of  $N_v$  (see Appendix). Fig. 3 shows the  $N_v = 8$  spectra which have been shifted and rescaled (by the same amount) to set the average level spacing of the edge states to  $\Delta = 1$ . This makes the resemblance with the spectrum of a chiral CFT very striking, where each “tower of states” corresponds to a WZW primary field and its descendants. Since the ES inherits from the spin-singlet character of the PEPS  $SU(2)$  Kramer degeneracies, the  $SU(2)_1$  CFT of the KL state is the most natural candidate. However, the  $SU(2)_1$  CFT has only two primary fields – the Identity and the Spinon fields – in disagreement with the plausible existence of four topological sectors for the  $d + id$  RVB. In addition, our numerical estimation of the conformal weight  $h_{1/2}$  of the Spinon sector (from the ratio of the lowest  $|S_z| = 1/2$  energy level to the  $|S_z| = 1$  one) gives  $h_{1/2} \simeq 0.93$  for  $N_v = 6$  and  $h_{1/2} \simeq 0.84$  for  $N_v = 8$ , significantly above the value  $h_{1/2} = 1/4$  for  $SU(2)_1$ .

*Entanglement Entropy and Hamiltonian* – We have computed the Von Neumann EE from the ES and results for the two topological sectors (with and without

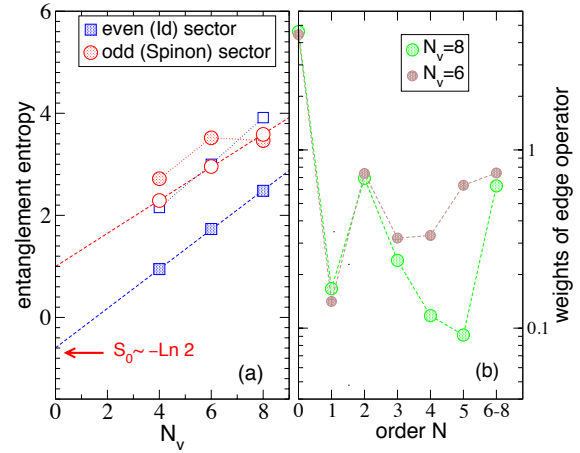


FIG. 4: (a) Entanglement entropy  $S$  vs cylinder perimeter in the two topological sectors with (open symbols) and without (full symbols)  $\mathbb{Z}_2$  flux (for  $\lambda_1 = \lambda_2 = \lambda_{\text{chiral}} = 1$ ). Linear fits (area law)  $S = aN_v + b$  are shown. (b) Weights vs  $N$  of the Entanglement Hamiltonian decomposed in terms of  $N$ -body contributions, for  $N_v = 6$  and  $N_v = 8$ .

$\mathbb{Z}_2$  flux) are shown in Fig. 4(a). In the Identity (integer spin) sector and no flux one can fit the EE according to the area law with a negative intercept  $b \sim -0.596$ . This value does not agree with the expected  $-\ln 2/2$  value for  $SU(2)_1$  but is close to  $-\ln 2 \sim 0.69$  also found in the critical RVB spin liquid [11]. To investigate the range of the EH we have decomposed it in terms of separate  $N$ -body terms whose weights can be computed. As can be shown in Fig. 4(b), the BH is long-range and retains a large weight on extended operators involving all the sites of the ring i.e. with  $N = N_v$ .

*Discussion and outlook* – It is well known in Particle Physics and lattice gauge theories (Nielsen and Ninomiya no-go theorem [33]) that a chiral field theory cannot be discretized on a lattice. This has brought some doubt in the community about the possibility of constructing a PEPS (of finite bond dimension  $D$ ) that could be the ground state of a local Hamiltonian within a topological chiral phase. Together with Ref. 25, the present work brings new perspectives : we have constructed a (two parameter) family of PEPS which are CSL with topological order and chiral edge modes and share some properties with the KL spin liquid state. Nevertheless, a precise identification of the PEPS was not possible and some differences with the KL state may arise : (i) First, once the time reversal is broken, the KL state is expected to have two-fold topological degeneracy on a torus. A priori, our CSL bears four topological sectors. The scaling of the relevant leading eigenvectors of the TM does not allow to safely conclude that two sectors only will survive in the thermodynamic limit. (ii) Our numerical simulations also point towards critical (singlet) correlations. This property may be closely related to the bi-

partiteness of the lattice and the existence of an effective field theory formulated in terms of height/gauge degrees of freedom [34]. Similar construction on non-bipartite lattice like the Kagome lattice (requiring larger bond dimension  $D > 3$ ) is left for future studies. (iii) Lastly, a precise assignment of the edge physics to a simple CFT was not possible, also calling for further studies. Deviations from a simple  $SU(2)_1$  CFT (expected for the KL state) may appear due to the critical property of the bulk. Finally, we note that PEPS construction of non-Abelian CSL with edge modes described by  $SU(2)_k$  CFT with  $k > 1$  would also be of great interest.

**Acknowledgment** – This project is supported by the NQPTP ANR-0406-01 grant (French Research Council). The numerical computations have been achieved at the CALMIP UV Supercomputer (Toulouse) and valuable help on the codes from Nicolas Renon is acknowledged. DP acknowledges illuminating discussions with Jérôme Dubail, Benoît Estienne, Pierre Pujol and Guifre Vidal as well as with the participants of the workshop “*Topological Phases and Quantum Computation*” (May 2014) at the Moorea Ecostation Center for Advanced Studies. JIC is partially supported by the EU project SIQS. NS acknowledges support by the Alexander von Humboldt foundation and the ERC grant WASCOSYS.

- 
- [1] Xiao-Gang Wen, Topological Orders and Chern-Simons Theory in strongly correlated quantum liquid, *Int. J. Mod. Phys. B* **5**, 1641 (1991).
- [2] A. Kitaev, *Ann. Phys.* **303**, 2 (2003), quant-ph/9707021.
- [3] Chetan Nayak, Steven H. Simon, Ady Stern, Michael Freedman, and Sankar Das Sarma, Non-Abelian anyons and topological quantum computation, *Rev. Mod. Phys.* **80**, 1083 (2008).
- [4] Immanuel Bloch, Jean Dalibard, and Sylvain Nascimbène, Quantum simulations with ultracold quantum gases, *Nature Physics*, **8**, 267 (2012).
- [5] F. Verstraete, V. Murg, and J. I. Cirac, *Adv. Phys.* **57**, 143 (2008), arXiv:0907.2796.
- [6] J. I. Cirac, D. Poilblanc, N. Schuch and F. Verstraete, Entanglement spectrum and boundary theories with projected entangled-pair states, *Phys. Rev. B* **83**, 245134 (2011).
- [7] Michael A. Levin and Xiao-Gang Wen, *Phys. Rev. B* **71**, 045110 (2005).
- [8] F. Verstraete, M. M. Wolf, D. Perez-Pérez-García and J. I. Cirac, *Phys. Rev. Lett.* **96**, 220601 (2006), quant-ph/0601075.
- [9] N. Schuch, D. Poilblanc, J. I. Cirac and D. Perez-García, Resonating valence bond states in the PEPS formalism, *Phys. Rev. B* **86**, 115108 (2012).
- [10] D. Poilblanc, N. Schuch, D. Perez-García and J. I. Cirac, Topological and entanglement properties of resonating valence bond wave functions, *Phys. Rev. B* **86**, 014404 (2012).
- [11] Ling Wang, Didier Poilblanc, Zheng-Cheng Gu, Xiao-Gang Wen and Frank Verstraete, Constructing gapless spin liquid state for the spin-1/2 J1-J2 Heisenberg model on a square lattice, *Phys. Rev. Lett.* **111**, 037202 (2013).
- [12] P. W. Anderson, Resonating valence bonds: A new kind of insulator?, *Mat. Res. Bull.* **8**, 153 (1973); P. W. Anderson, The resonating valence bond state in  $\text{La}_2\text{CuO}_4$  and superconductivity, *Science* **235**, 1196 (1987).
- [13] X. G. Wen, Chiral Luttinger liquid and the edge excitations in the fractional quantum Hall states, *Phys. Rev. B* **41**, 12838 (1990).
- [14] For a review on CFTs see e.g. Paul Ginsparg, Applied Conformal Field Theory, in *Fields, Strings and Critical Phenomena*, Les Houches Summer School, North-Holland, Eds. E. Brézin and J. Zinn-Justin (1988); arXiv:hep-th/9108028.
- [15] R. B. Laughlin, *Phys. Rev. B* **23**, 5632 (1981).
- [16] G. Moore and N. Read, Nonabelions in the fractional quantum Hall effect, *Nuclear Physics B* **360**, 362 (1991).
- [17] N. Read and E. Rezayi, Beyond paired quantum Hall states: parafermions and incompressible states in the first excited Landau level, *Phys. Rev. B* **59**, 8084 (1999).
- [18] V. Kalmeyer and R. B. Laughlin, Equivalence of the resonating-valence-bond and fractional quantum Hall states, *Phys. Rev. Lett.* **59**, 2095 (1987).
- [19] Xiao-Gang Wen, F. Wilczek, and A. Zee, Chiral Spin States and Superconductivity, *Phys. Rev. B* **39**, 11413 (1989).
- [20] B. Bauer, L. Cincio, B. P. Keller, M. Dolfi, G. Vidal, S. Trebst, and A. W. W. Ludwig, Chiral spin liquid and emergent anyons in a Kagome lattice Mott insulator, *Nature Communications* **5**, 5137 (2014).
- [21] Anne E. B. Nielsen, German Sierra, J. Ignacio Cirac, Fractional quantum Hall states in lattices: Local models and physical implementation, *Nature Communications* **4**, 2864 (2013)
- [22] Shou-Shu Gong, Wei Zhu, and D. N. Sheng, Emergent Chiral Spin Liquid: Fractional Quantum Hall Effect in a Kagome Heisenberg Model, *Scientific Reports* **4**, 6317 (2014).
- [23] J. Dubail and N. Read, Tensor network trial states for chiral topological phases in two dimensions, arXiv:1307.7726.
- [24] T. B. Wahl, H.-H. Tu, N. Schuch, and J. I. Cirac, Projected entangled-pair states can describe chiral topological states, arXiv:1308.0316.
- [25] Shuo Yang, Thorsten B. Wahl, Hong-Hao Tu, Norbert Schuch, and J. Ignacio Cirac, Chiral projected entangled-pair state with topological order, arXiv:1411.6618.
- [26] A. F. Albuquerque and F. Alet, Critical correlations for short-range valence-bond wavefunctions on the square lattice, *Phys. Rev. B* **82**, 180408R (2010).
- [27] Y. Tang, A. W. Sandvik and C. L. Henley, Properties of resonating valence bond spin liquids and critical dimer models, *Phys. Rev. B* **84**, 174427 (2011).
- [28] L. Landau et E. Lifchitz, *Physique Théorique Tome III, Mécanique Quantique, Troisième Edition*, Editions Mir (Moscou), p. 435 (1975).
- [29] One could equivalently re-write the same PEPS using new  $R_a$  and  $I$  tensors belonging to the  $A_1$  (s-wave) and  $A_2$  (g-wave) IRREP, respectively, via a simple gauge transformation.
- [30] Norbert Schuch, Didier Poilblanc, J. Ignacio Cirac, and David Perez-García, Topological order in PEPS: Transfer operator and boundary Hamiltonians, *Phys. Rev. Lett.* **111**, 090501 (2013).

- [31] Under  $180^\circ$ -spin rotation on the B sublattice, the  $S_z^{\text{bra}}$  and  $S_z^{\text{ket}}$  components transform into *staggered* components.  $|S_z^{BK}|$  is preserved under translation around the ring so that the momentum  $K$  and  $|S_z^{BK}|$  can be used simultaneously to block diagonalize the TM.
- [32] For the NN RVB state on the square lattice, the number of  $|0\rangle$  itself is conserved. It is a consequence of the

- existence of longer-range singlets (when  $\lambda_2 \neq 0$  and/or  $\lambda_{\text{chiral}} \neq 0$ ) that only the parity is conserved.
- [33] H. B. Nielsen and M. Ninomiya, Nucl. Phys. B **193**, 173 (1981).
- [34] R. Moessner, S. L. Sondhi, and E. Fradkin, Phys. Rev. B **65**, 024504 (2002).

## Appendices

### DERIVATION OF THE PEPS ANSATZ.

Here we wish to construct a modified RVB *complex* singlet wavefunction whose real and imaginary components transform according to different irreducible representations (IRREP)  $\mathcal{R}_1$  and  $\mathcal{R}_2$  of the  $C_{4v}$  point group of the square lattice [28]. More precisely, (i) the wavefunction should have the form  $|\Psi\rangle = |\Psi_{\mathcal{R}_1}\rangle + i|\Psi_{\mathcal{R}_2}\rangle$ , where  $|\Psi_{\mathcal{R}_1}\rangle$  and  $|\Psi_{\mathcal{R}_2}\rangle$  are assumed to be real (and non-zero), and (ii)  $\mathcal{R}_1$  and  $\mathcal{R}_2$  have to be such that, under any reflection symmetry of  $C_{4v}$ ,  $|\Psi\rangle$  transforms into  $|\Psi^*\rangle$ , its time-reversed state (possibly up to a sign), which is indeed a necessary condition for a chiral spin liquid. With PEPS, one can achieve exactly this goal by enforcing symmetries at the level of the tensor itself. Let us write  $A = R + iI$ , where  $R$  and  $I$  are two real tensors. We impose that  $R$  and  $I$  transform, under point group operations, according to the  $\mathcal{T}_1 = B_1$  ( $d_{x^2-y^2}$  orbital symmetry) and  $\mathcal{T}_2 = B_2$  ( $d_{xy}$  orbital symmetry) IRREPs, respectively. In that case, it is easy to see (see main text) that the real and imaginary parts of the wavefunction (on a  $L \times L$  torus) transform according to the  $\mathcal{R}_1 = A_1$  (s-wave) and  $\mathcal{R}_2 = A_2$  (g-wave) IRREP of  $C_{4v}$ .

Hence, we require that the  $R$  and  $I$  components of the  $A$  tensor follow,

$$R_{lurd}^s = R_{ldru}^s = R_{ruld}^s = -R_{drul}^s = -R_{uldr}^s, \quad (2)$$

$$I_{lurd}^s = -I_{ldru}^s = -I_{ruld}^s = I_{drul}^s = I_{uldr}^s. \quad (3)$$

Here  $l, u, r$  and  $d$  label the bond variables (0,1, and 2 for the  $|\uparrow\rangle, |\downarrow\rangle$  and  $|0\rangle$  virtual states, respectively) clockwise around the site, starting from its left bond, and  $s = 0, 1$  is the physical index. To solve these equations one has to go through all possible combinations of the bond indices  $l, u, r$  and  $d$ . One obtains,

$$R_{2s22}^{s'} = \lambda_1^{ss'}, \quad (4)$$

$$R_{222s}^{s'} = \lambda_1^{ss'}, \quad (5)$$

$$R_{22s2}^{s'} = -\lambda_1^{ss'}, \quad (6)$$

$$R_{s222}^{s'} = -\lambda_1^{ss'}. \quad (7)$$

In fact, spin SU(2)-invariance implies that,

$$\lambda_1^{ss'} = \delta_{ss'} \lambda_1. \quad (8)$$

These tensor elements correspond exactly to those of the NN RVB wavefunction. Note that the tensor elements of  $I$  with the same indices identically vanish by symmetry. The solution of Eqs. (2) and (3) gives also non-zero tensor elements that correspond to quantum teleportation via diagonal bonds,

$$R_{s\bar{s}s2}^{s'} = \lambda_0^{ss'}, \quad (9)$$

$$R_{s2s\bar{s}}^{s'} = \lambda_0^{ss'}, \quad (10)$$

$$R_{2s\bar{s}s}^{s'} = -\lambda_0^{ss'}, \quad (11)$$

$$R_{\bar{s}s2s}^{s'} = -\lambda_0^{ss'}, \quad (12)$$

where  $\lambda_0^{ss'} \in \mathbb{R}$ . One also gets (grouping the  $R$  and  $I$  tensors),

$$A_{s\bar{s}s2}^{s'} = \lambda_2^{ss'} + i\lambda_{\text{chiral}}^{ss'}, \quad (13)$$

$$A_{\bar{s}s2s}^{s'} = \lambda_2^{ss'} + i\lambda_{\text{chiral}}^{ss'}, \quad (14)$$

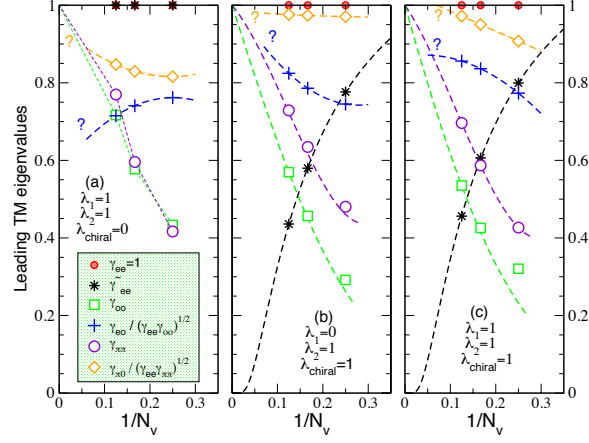


FIG. 5: Finite size scaling of the leading eigenvalues of the diagonal blocks ( $\Gamma_{ee}$  and  $\Gamma_{oo}$ ) and of the off-diagonal blocks ( $\tilde{\Gamma}_{ee}$  and  $\Gamma_{eo}$ ) of the transfer matrix (after proper normalization). Same notation as Fig. 2(b) in the main text. The three panels correspond to different choices of the parameters of the PEPS as indicated on the plot. (a) is a non-chiral RVB state ( $\tilde{\gamma}_{ee} = 1$ ), (b) does not contain NN valence bonds and (c) is a repetition of Fig. 2(b) for convenience.

$$A_{s2\bar{s}s}^{s'} = \lambda_2^{ss'} - i\lambda_{\text{chiral}}^{ss'}, \quad (15)$$

$$A_{\bar{s}ss2}^{s'} = \lambda_2^{ss'} - i\lambda_{\text{chiral}}^{ss'}, \quad (16)$$

$$A_{ss2\bar{s}}^{s'} = -\lambda_2^{ss'} + i\lambda_{\text{chiral}}^{ss'}, \quad (17)$$

$$A_{2\bar{s}ss}^{s'} = -\lambda_2^{ss'} + i\lambda_{\text{chiral}}^{ss'}, \quad (18)$$

$$A_{s\bar{s}2s}^{s'} = -\lambda_2^{ss'} - i\lambda_{\text{chiral}}^{ss'}, \quad (19)$$

$$A_{2ss\bar{s}}^{s'} = -\lambda_2^{ss'} - i\lambda_{\text{chiral}}^{ss'}, \quad (20)$$

where  $\lambda_2^{ss'}, \lambda_{\text{chiral}}^{ss'} \in \mathbb{R}$  are independent constants and  $\bar{s}$  is the time-reversed of the spin  $s$ .

Finally, enforcing the invariance under  $SU(2)$  spin-rotations (singlet character of the PEPS) one finds that  $\lambda_2^{ss'}$  ( $\lambda_{\text{chiral}}^{ss'}$  and  $\lambda_0^{ss'}$ ) is (are) diagonal in the spin indices and even (odd) under spin inversion,

$$\lambda_2^{ss'} = \delta_{ss'} \lambda_2, \quad (21)$$

$$\lambda_{\text{chiral}}^{ss'} = \delta_{ss'} (-1)^s \lambda_{\text{chiral}}, \quad (22)$$

$$\lambda_0^{ss'} = \delta_{ss'} (-1)^s \lambda_0. \quad (23)$$

Note that spin rotation invariance leads also to the relation,

$$\lambda_0 = 2\lambda_2. \quad (24)$$

### LEADING TM EIGENVALUES: COMPARISON BETWEEN DIFFERENT WAVE FUNCTIONS.

We compare the finite size scalings of the LE of the TM for three choices of the tensor parameters in Fig. 5 corresponding to the critical (non-chiral) RVB state in (a) and chiral topological liquids in (b) and (c). For all wave functions, the finite size scalings are consistent with  $\gamma_{oo} \rightarrow 1$  and  $\gamma_{\pi\pi} \rightarrow 1$ . However, in (b) and (c) it is difficult to assess with full confidence that  $\gamma_{\pi 0}/(\gamma_{ee}\gamma_{\pi\pi})^{1/2}$  and  $\gamma_{eo}/(\gamma_{ee}\gamma_{oo})^{1/2}$  *do not* go to exactly 1 when  $N_v \rightarrow \infty$ , as required to obtain separate topological sectors.

### ENTANGLEMENT SPECTRUM: COMPARISON BETWEEN DIFFERENT SIZES.

Comparisons between ES for cylinders with different perimeters is shown in Fig. 6(a-c). Remarkably the slope of the chiral edge modes is very similar for  $N_v = 6$  and  $N_v = 8$ .

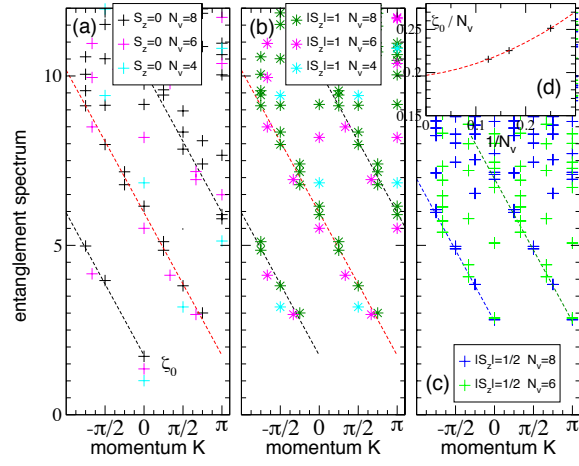


FIG. 6: Entanglement Spectrum vs momentum along the edge for  $N_v = 4, 6, 8$  (for  $\lambda_1 = \lambda_2 = \lambda_{\text{chiral}} = 1$ ). (a), (b) and (c) show  $S_z = 0$ ,  $|S_z| = 1$  and  $|S_z| = 1/2$ , respectively. The dashed lines show a fit of the chiral edge modes for  $N_v = 8$ . (d) Finite size scaling of the lowest eigenvalue of the ES.